ARTICLE

Mutations in FAM20C Are Associated with Lethal Osteosclerotic Bone Dysplasia (Raine Syndrome), Highlighting a Crucial Molecule in Bone Development

M. A. Simpson, R. Hsu, L. S. Keir, J. Hao, G. Sivapalan, L. M. Ernst, E. H. Zackai, L. I. Al-Gazali, G. Hulskamp, H. M. Kingston, T. E. Prescott, A. Ion, M. A. Patton, V. Murday, A. George, and A. H. Crosby

The generation and homeostasis of bone tissue throughout development and maturity is controlled by the carefully balanced processes of bone formation and resorption. Disruption of this balance can give rise to a broad range of skeletal pathologies. Lethal osteosclerotic bone dysplasia (or, Raine syndrome) is an autosomal recessive disorder characterized by generalized osteosclerosis with periosteal bone formation and a distinctive facial phenotype. Affected individuals survive only days or weeks. We have identified and defined a chromosome 7 uniparental isodisomy and a 7p telomeric microdeletion in an affected subject. The extent of the deleted region at the 7p telomere was established by genotyping microsatellite markers across the telomeric region. The region is delimited by marker *D7S2563* and contains five transcriptional units. Sequence analysis of *FAM20C,* located within the deleted region, in six additional affected subjects revealed four homozygous mutations and two compound heterozygotes. The identified mutations include four nonsynonymous base changes, all affecting evolutionarily conserved residues, and four splice-site changes that are predicted to have a detrimental effect on splicing. FAM20C is a member of the FAM20 family of secreted proteins, and its mouse orthologue (DMP4) has demonstrated calcium-binding properties; we also show by in situ hybridization its expression profile in mineralizing tissues during development. This study defines the causative role of FAM20C in this lethal osteosclerotic disorder and its crucial role in normal bone development.

The sclerosing bone dysplasias are an extended heterogeneous group of predominantly inherited conditions characterized by abnormal hardening and increase in density of bone.[1] The neonatal osteosclerotic dysplasias, which include lethal osteosclerotic bone dysplasia, are set apart because of their aggressive nature and early onset.[1] The first reported case of lethal osteosclerotic bone dysplasia, also commonly referred to as "Raine syndrome" (MIM 259775), was presented in 1989, a female neonate, born at term, who died at age 86 min.[2] Since this original report, an additional 13 cases have been described.[3–11] Affected individuals survive only days or weeks, with the cause of death most commonly reported as respiratory failure, which may be due to thoracic malformation. Radiographic studies have shown generalized increase in the density of all bones and marked increase in the ossification of the skull.[12] The increased ossification of the basal structures of the skull and the facial bones underlies the characteristic facial features, which include narrow prominent forehead, proptosis of the eyes, depressed nasal bridge, and midfacial hypoplasia. Periosteal bone formation is also characteristic of this disorder and differentiates it from osteopetrosis and other known lethal and nonlethal osteosclerotic bone dysplasias.[9] The periosteal bone formation typically extends along the diaphysis of long bones, adjacent to areas of cellular soft tissue.[11]

Raine syndrome appears to be inherited in an autosomal recessive fashion, since many of the reported case patients are the offspring of consanguineous unions, and recurrence in siblings has also been reported.[9,11] In the current study, we identified an unusual chromosome 7 rearrangement and microdeletion in an affected subject and subsequently identified mutations in the *FAM20C* gene (MIM *611061), located within the deleted region, in six additional affected subjects.

Material and Methods

Sample Ascertainment

We studied seven unrelated affected individuals and samples from the parents of three of the affected individuals. Three subjects were the offspring of consanguineous unions. All subjects presented at birth with features consistent with the diagnosis of

From the Department of Medical Genetics, Clinical Developmental Sciences, St George's University of London, London (M.A.S.; R.H.; L.S.K.; G.S.; A.I.; M.A.P.; A.H.C.); Department of Oral Biology, University of Illinois at Chicago, Chicago (J.H.; A.G.); Department of Pathology and Laboratory Medicine (L.M.E.) and Division of Human Genetics (E.H.Z.), Children's Hospital of Philadelphia, and University of Pennsylvania School of Medicine (L.M.E.), Philadelphia; Department of Paediatrics, Faculty of Medicine and Health Sciences, United Arab Emirates University, Al Ain, United Arab Emirates (L.I.A.G.); Klinik und Poliklinik für Kinderheilkunde, Westfälsche Wilhelms-Universität Münster, Münster, Germany (G.H.); Regional Genetic Service, St Mary's Hospital, Manchester, United Kingdom (H.M.K.); Department of Medical Genetics, Rikshospitalet University Hospital, Oslo (T.E.P.); and Department of Clinical Genetics, Royal Hospital for Sick Children, Glasgow (V.M.)

Received June 11, 2007; accepted for publication July 10, 20007; electronically published September 14, 2007.

Address for correspondence and reprints: Dr. Andrew Crosby, Department of Medical Genetics, St George's University of London, Cranmer Terrace, London SW17 0RE, United Kingdom. E-mail: acrosby@sgul.ac.uk

Am. J. Hum. Genet. 2007;81:906–912. © 2007 by The American Society of Human Genetics. All rights reserved. 0002-9297/2007/8105-0005$15.00
DOI: 10.1086/522240

Raine syndrome and died within the first few weeks of life. Samples for blood and/or skin biopsy were obtained after appropriate informed consent was given by the parents.

Cytogenetic Analysis

Chromosomal analysis was performed on 24–48 h–synchronized cell cultures. Karyotyping was performed using standard trypsin-Giemsa staining. FISH was performed according to standard protocols. The RP11-90P13 chromosome 7 telomeric probe and a chromosome 7 centromeric probe were directly labeled with fluorochromes. Probes were denatured at 80°C for 5 min and were preannealed for 2 h at 37°C with a 50-fold excess of both Cot-1 DNA (Life Technologies) and DNA from human placenta (Sigma).

Genotyping and Sequence Analysis

Genotypes of microsatellite markers were determined by PCR amplification and subsequent analysis by PAGE and were visualized by silver staining. Intronic, exon-flanking primers were designed to amplify all 10 exons and associated splice junctions of *FAM20C*. PCR-amplified fragments were purified using QIAquick PCR cleanup columns (QIAGEN) and were sequenced using the BigDye terminator chemistry (v. 3.5) (Applied Biosystems) on an ABI3100 genetic analyzer (Applied Biosystems). Sequences were aligned and compared with reference sequences with use of SeqScape software (v. 2.0) (Applied Biosystems).

Bioinformatic Analysis

Cross-species sequence alignments were performed using the ClustalW program.[13] Analysis of splice-site variants was performed using the Automated Splice Site–Analysis Server.[14]

In Situ Hybridization

The full-length mouse *FAM20C* (DMP4) cDNA was linearized for in vitro transcription with use of appropriate enzymes. The antisense and sense samples complementary to target mRNA were prepared by in vitro transcription with use of T3 or T7 polymerase (Promega) with ^{35}S-labeled dUTP (ICN). Briefly, tissues from embryonic day 15 (E15) and postnatal day 1 (P1) mice were fixed overnight with 4% paraformaldehyde in PBS (pH 7.4) at 4°C, were washed overnight with PBS at 4°C, and were dehydrated and embedded in paraffin. Sections (5 μm) were cut, were mounted on charged glass slides, were dewaxed in xylene, and were rehydrated. After the sections were washed in PBS, they were digested with 200 mU/ml proteinase K, were postfixed, and were acetylated with 0.25% acetic anhydride. The sections were hybridized overnight at 55°C with radiation-labeled riboprobes. The sections were then washed with 50% formamide, 2 × SSC (0.3 M NaCl containing 0.03 M sodium citrate) for 30 min at 55°C, were digested with RNase A, and were washed once with 2 × SSC and twice with 0.2 × SSC for 20 min at 55°C. The signal was visualized with NBT2 silver; then, the slides were counterstained with hematoxylin and were dehydrated and mounted.

RNA Isolation, RT-PCR, and Northern-Blot Analysis

Total RNA from adult mouse tissues was isolated. For RT-PCR, 3 μg of total RNA was reverse transcribed for 90 min at 42°C with Superscript II (GIBCO/BRL). PCR Supermix (GIBCO/BRL) was used in the PCR. For northern blotting, 10 μg total RNA was fractionated by electrophoresis through 0.8% agarose gels containing formaldehyde and were blotted onto Hybond nylon membrane (Amersham Biosciences). Full-length mouse *FAM20C* (DMP4) cDNA was labeled with [-P]dCTP with use of a random labeling system (Ambion). Hybridization was performed in ExpressHyb hybridization buffer (Clontech) at 68°C. Membranes were washed twice with 2 × SSC, 0.1% SDS, at 42°C for 20 min and twice in 0.1 × SSC, 0.1% SDS, at 56°C for 30 min, and were exposed overnight to x-ray film at −80°C.

Results

Cytogenetic examination by Giemsa staining of a sample from a previously unreported male child with lethal osteosclerotic bone dysplasia, who died 2 h after birth, revealed the presence of a pseudodicentric chromosome 7 (fig. 1*a*) with the karyotype 45, XY psudic (7;7) (p22;p22). Analysis of parental chromosomes revealed normal karyotypes. Hybridization with a chromosome 7p telomeric FISH probe (RP11-90P13) confirmed the deletion of the terminal portions of 7p at the fusion point of the pseudodicentric chromosome (fig. 1*b*). Genotyping of microsatellite markers located across chromosome 7 revealed uniparental isodisomy, with paternal origin of the two copies of chromosome 7 present within the pseudodicentric chromosome (data not shown).

The child was born at 37 wk of gestation; at birth, the child breathed independently but developed respiratory distress. Despite medical intervention to improve respiration, the patient died 3 h after delivery. Postmortem examination revealed the presence of multiple congenital abnormalities consistent with a Raine syndrome diagnosis: prominent forehead, short neck, proptosis, midfacial hypoplasia, and a depressed nasal bridge (table 1, subject 1). Radiological investigation revealed diffuse osteosclerosis, with irregular periosteal bone formation along the clavicles and ribs. The skull had wide cranial sutures with evidence of premature closure, whereas the base of the skull showed an increased thickness of all bony landmarks.

The extent of the deleted region of the 7p telomere was established by genotyping microsatellite markers across the telomeric region. Markers *D7S2477* and *D7S1484* are contained within the deleted region and therefore were absent in the affected subject. The next-most-distal marker on chromosome 7p, *D7S2563,* positioned proximal to *D7S1484,* was successfully amplified from the DNA of the affected subject and displayed a genotype consistent with uniparental isodisomy (data not shown). The region distal to *D7S2563* was therefore considered a candidate for the region containing the causative gene in this disorder. A continuous human sequence across this region was only recently completed with the alternative assembly NT_079592 (GenBank) (fig. 1*c*). The region contains just five known or predicted genes: *FLJ45445,* which has an unclassified transcription discrepancy; *LOC730345, LOC730346,* and *LOC651986,* which are derived by automated computational analysis; and *FAM20C,* a 10-exon

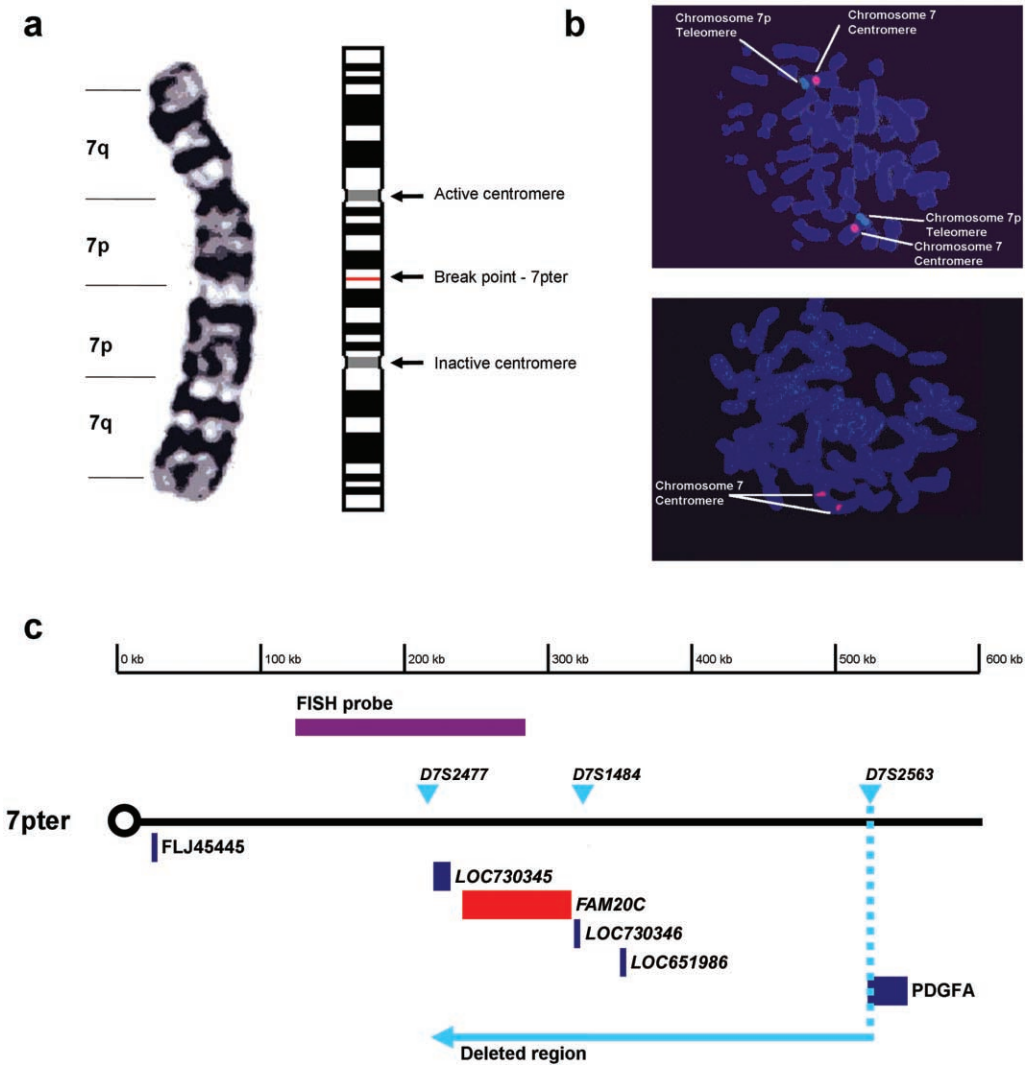

Figure 1. *a,* G banding of the pseudodicentric chromosome 7. *b,* FISH staining with probes directed against chromosome 7 centromere (*pink*) and chromosome 7p telomere (*blue*). The upper panel displays a normal karyotype from the affected child's father, and the lower panel is from the affected child, with an absence of signal from the chromosome 7pter probe. *c,* Schematic representation, from contig NT_079592 (GenBank), of the terminal region of chromosome 7p, including the location of the deleted 7pter FISH probe. Marker *D7S2563* delimits the deleted region, which contains five potential transcriptional units.

gene that represents the most telomeric confirmed gene model on chromosome 7p.

The previous study of *FAM20C,*[15] as well as our recent studies of its mouse orthologue (DMP4),[16] identified this gene as an excellent candidate in the pathogenesis of this disorder. The coding regions and associated splice sites of this gene were therefore sequenced in a cohort of six affected subjects (three presented elsewhere in clinical case reports[3,10,11] and three previously unreported additional subjects affected with lethal osteosclerotic bone dysplasia) and three sets of parents. (An overview of clinical features is presented in table 1.) Sequence variations consistent with autosomal recessive inheritance were identified in all six subjects (fig. 2). Homozygous changes were identified in four subjects, three of whom were the offspring of consanguineous unions, and comprised three nonsynonymous base changes (1093G→A [Gly365Arg[, 1121T→G [Leu374-Arg], and 1603C→T [Arg535Trp]) and an intron 4/exon 5 acceptor splice-site change (c915-3C→G). Two compound heterozygotes were also identified in affected subjects with no evidence of parental consanguinity—one heterozygous for a nonsynonymous base change (1094G→A [Gly365-Glu]) and an intron 7/exon 8 acceptor splice-site change (c1322-2A→G) and the second with heterozygous variants in the exon 4/intron 4 donor splice site (c914+5G→C) and an intron 8/exon 9 acceptor splice site (c1404-1G→A). In the three cases where parental DNA was available, the parents were found to be heterozygous for the respective variants (data not shown). The eight variants identified were not present in at least 300 control chromosomes.

Table 1. Clinical Features and Mutations Identified for Subjects with Raine Syndrome

Subject	Chromosomal Abnormality or Mutation(s) in *FAM20C*	Sex	Consanguinity	Gestation (wk)	Survived >10 d	Osteosclerosis	PBF[a]	Cerebral Calcifications	Thoracic Hypoplasia	Pulmonary Hypoplasia	Case Report
1	45,XY psudic (7;7) (p22;p22)	M	−	37	−	+	+	U	+	+	
2	1603C→T (Arg535Trp)	M	+	37	−	+	+	U	+	−	Kingston et al.[3]
3	1093G→A (Gly365Arg)	M	+	38	−	+	+	U	+	+	
4	c915-3C→G	M	−	36	+	+	+	−	+	−	Al-Gazali et al.[10]
5	1121T→G (Leu374Arg)	F	+	32	−	+	+	+	+	+	Hulskamp et al.[11]
6	1094G→A (Gly365Glu) and c1322-2A→G	F	−	38	+	+	+	+	−	−	
7	c914+5G→C and c1404-1G→A	F	−	32	−	+	+	+	+	+	

NOTE.—All subjects had prominent forehead, proptosis, midfacial hypoplasia, and depressed nasal bridge. A plus sign (+) = present; a minus sign (−) = absent; U = unknown status.

[a] PBF = periosteal bone formation.

FAM20C orthologues are found in a range of species. Cross-species alignment of their protein sequences reveals a high level of evolutionary conservation. Human and mouse (DMP4) sequences display 85% identity and 91% similarity, and similarly high levels are seen across other species (fig. 2). The N-terminal region contains a signal peptide sequence that shows moderate conservation across all species analyzed. However, it is the C-terminal half of the protein that displays the highest level of conservation. This region has been termed the "conserved C-terminal domain" (CCD), and its sequence structure overlaps the DUF1193 domain.[15] The 3-aa residues altered by the four nonsynonymous base changes identified in affected subjects are all evolutionarily conserved residues within the CCD.

Individual information analysis of the four identified splice-site variants suggests that each mutation has a weakening effect on splice-site binding. (See fig. 2 for calculated R_i and Z scores.) Three of the variants (c914+5G→C, c915-3C→G, and c1322-2A→G) greatly weaken the splice site predicted by the Automated Splice Site–Analysis Server,[14] and the fourth (c1404-1G→A) is predicted to completely abolish splicing at this junction. The donor-site mutation (c914+5G→C) in the exon 4/intron 4 splice junction reduces the R_i score from 10.7 to 6.8 bits, which typically would lead to the prediction of a leaky mutation. However, this splice site is located within a common polymorphic 34-bp repeat (911_c914+30dup) consisting of the last 4 bases of exon 4 and the first 30 bases of intron 4. The c914+5G→C mutation is located on a chromosome with a 68-bp allele containing two copies of the repeat; therefore, a pre-existing 10.7-bit cryptic splice site exists 34 bases downstream from the mutated junction, which is therefore likely to be preferentially employed for splicing.

The identification of mutations in *FAM20C* in affected patients highlights a crucial role of this molecule in the development of mineralized tissue. The expression pattern of the mouse *FAM20C* orthologue (DMP4) during development was investigated by situ hybridization in sagittal sections of E15 (whole body) and P1 (head) mice. Notably, strong expression was observed within chondroblasts of the developing somites and limb girdle in the E15 mouse (fig. 3*a*). Sections of alveolar bone in P1 mice revealed expression in osteoblasts and ameloblasts and particularly strong expression in odontoblasts at this early stage of predentine mineralization (fig. 3*b*). RT-PCR amplification and the detection of a single transcript of ~3 kb by northern-blot analysis verified the presence of *FAM20C* (DMP4) in both long bone and tooth germ (fig. 3*c*).

Discussion

The recessive expression of the mutations identified and the fact that they are predicted either to alter evolutionarily conserved amino acids or to have a strong detrimental effect on splicing, taken together with the telomeric deletion containing the *FAM20C* gene, strongly suggest that loss of function of this protein is responsible for the disease phenotype. Despite the spectrum of mutations identified in *FAM20C* in the six subjects and a telomeric deletion of the region containing the gene in another, correlation between genotype and phenotype is hindered by the complexity and severity of Raine syndrome presentations. Whereas there is some variation in presentation and length of survival, correlation to genotype is complicated by the small number of cases, limited clinical information, and different therapeutic interventions. However, it does not appear that there is any clear correlation between the severity of presentation and the type of mutation (i.e., splice site or missense), and the compound heterozygous subjects are as profoundly affected as are the homozygous subjects. Interestingly, the deleted region in patient 1, delimited by marker *D7S2563,* contains four additional putative genes. However, the phenotype in this case is characteristic of Raine syndrome, and none of the features of this subject appear to be unique and all have been reported in previous cases, although the severity of the phenotype could easily mask any additional effects of the deletion of these genes.

FAM20C was reported as a member of the evolutionarily conserved FAM20 family of secreted proteins that show sequence similarity to FAM20A (MIM *611062), which was identified through its differential expression during hematopoietic differentiation.[15] We have recently shown that overexpression of the mouse homologue of this gene accelerates the odontoblast differentiation process and mineralized nodule formation and that in vitro silencing by RNA interference inhibits odontoblast differentiation and

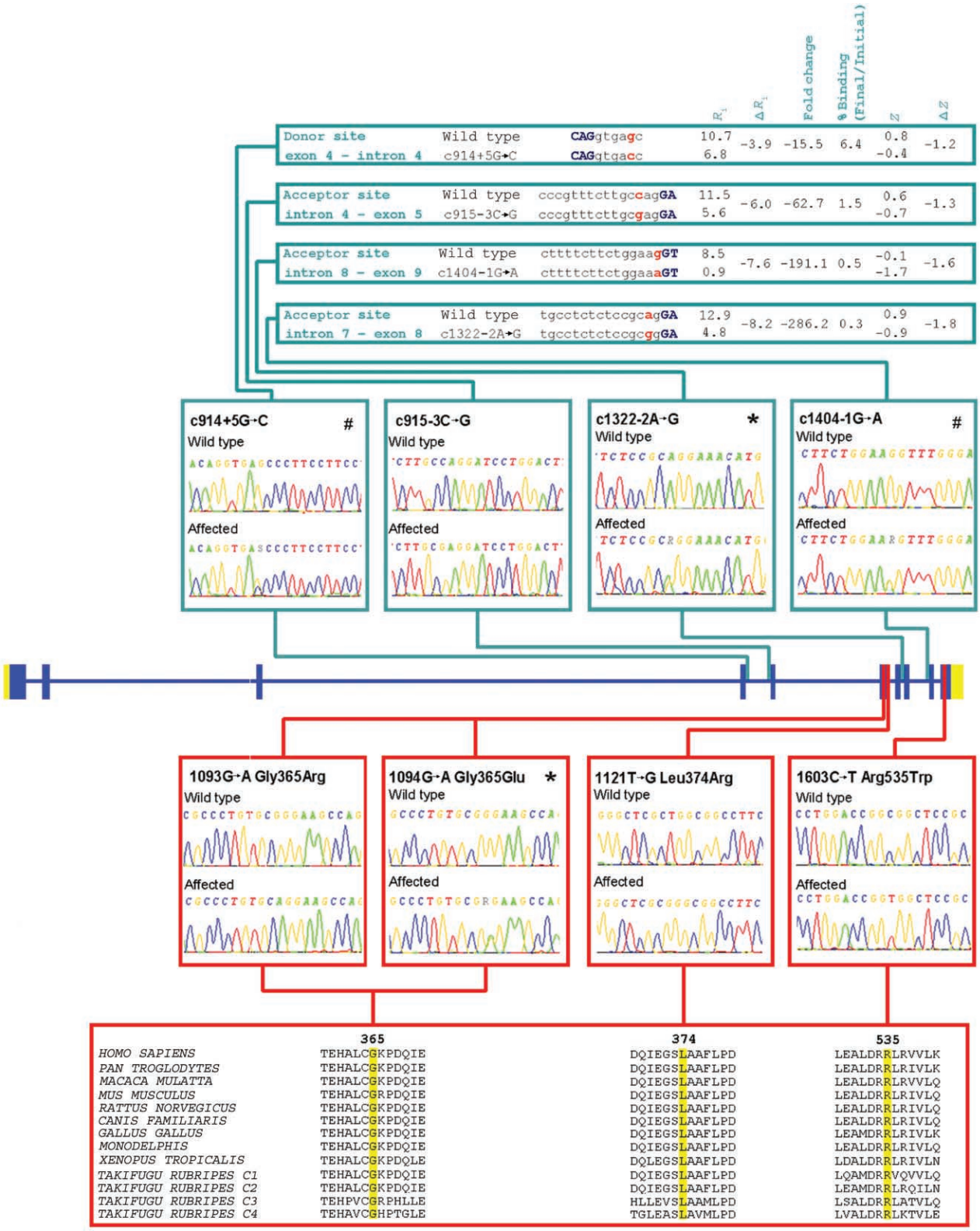

Figure 2. Sequence chromatograms, predicted effects, and locations of the mutations identified in the six additional affected individuals. Mutations are present in affected individuals as homozygotes, apart from two compound heterozygotes (c914+5G→C, c1401-1G→A, designated by a number sign [#], and 1094G→A, c1322-2A→G, designated by an asterisk [*]). Statistical analysis of each of the splice-site variants is displayed above the chromatograms (*blue path*). Also shown is a schematic representation of multiple-species sequence alignment of the FAM20C protein sequences affected by respective variants (*red path*).

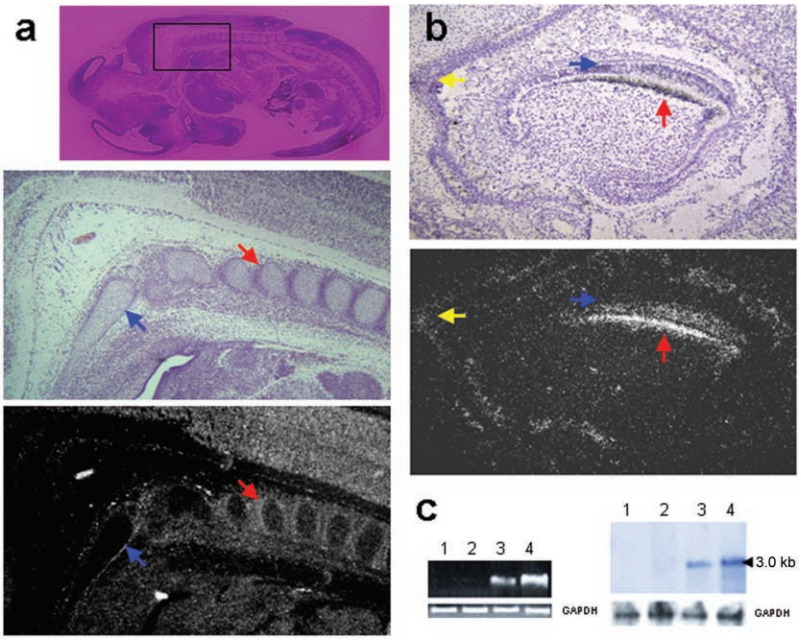

Figure 3. *a,* In situ hybridization of the mouse FAM20C orthologue (DMP4) on E15 mouse, with light microscopy and dark field images showing the developing vertebral column with expression on the mineralizing surface of somites (*red arrow*) and limb girdle (*blue arrow*). *b,* Light microscopy and dark field images showing expression of FAM20C (DMP4) in osteoblasts (*yellow arrow*), odontoblasts (*red arrow*), and ameloblasts (*blue arrow*) of the alveolar bone in a P1 mouse. *c,* PCR analysis of *Fam20C* (DMP4) mRNA from multiple tissues from a P5 SD rat (1 = spleen, 2 = skeletal muscle, 3 = bone, and 4 = tooth germ) (*left*). Glyceraldehyde-3-phosphate dehydrogenase (GAPDH) is used as an internal control. *Right,* With northern-blot analysis, 20 μg of total RNA isolated from P5 rats (1 = spleen, 2 = skeletal muscles, 3 = bones, and 4 = tooth germs), was electrophoresed, blotted, and probed for *FAM20C* (DMP4). The blot was stripped and reprobed for GAPDH.

mineralization.[16] We also showed that this molecule binds calcium and that a conformational change in the protein is associated with this interaction.[16] Interestingly, reduced serum calcium levels have been reported in lethal osteosclerotic bone dysplasia, although urinary excretion of calcium and phosphate has been within the normal range for the same subjects.[11] The formation of calcified tissue is a well-regulated process, with a complex interplay between both promoters and inhibitors of mineralization. Although more-detailed further investigations are required, the apparent contradiction between the proposed loss-of-function mutations reported in this study and the mineralization-promoting properties of FAM20C in vitro may reflect the conformational change of FAM20C in the presence of excess calcium.[16] The identification of *FAM20C* as the gene responsible for the increase in bone density and appositional bone formation that underlies this lethal human disease defines a critical component in the growing list of molecules known to be involved in bone development and mineralization.

Acknowledgments

We thank the families of all the affected subjects, for their participation, and Birth Defects Foundation UK, for financial support.

Web Resources

The accession number and URLs for data presented herein are as follows:

GenBank, http://www.ncbi.nlm.nih.gov/Genbank/ (for *Homo sapiens* chromosome 7 genomic contig [accession number NT_079592])

Online Mendelian Inheritance in Man (OMIM), http://www.ncbi.nlm.nih.gov/Omim/ (for Raine syndrome, *FAM20C,* and FAM20A)

References

1. Superti-Furga A, Unger S (2007) Nosology and classification of genetic skeletal disorders: 2006 revision. Am J Med Genet A 143:1–18
2. Raine J, Winter RM, Davey A, Tucker SM (1989) Unknown syndrome: microcephaly, hypoplastic nose, exophthalmos, gum hyperplasia, cleft palate, low set ears, and osteosclerosis. J Med Genet 26:786–788
3. Kingston HM, Freeman JS, Hall CM (1991) A new lethal sclerosing bone dysplasia. Skeletal Radiol 20:117–119
4. Kan AE, Kozlowski K (1992) New distinct lethal osteosclerotic bone dysplasia (Raine syndrome). Am J Med Genet 43:860–864
5. Patel PJ, Kolawole TM, al Mofada S, Malabarey TM, Hulailah A (1992) Osteopetrosis: brain ultrasound and computed tomography findings. Eur J Pediatr 151:827–828

6. Al Mane KA, Coates RK, McDonald P (1996) Intracranial calcification in Raine syndrome. Pediatr Radiol 26:55–58
7. Rejjal A (1998) Raine syndrome. Am J Med Genet 78:382–385
8. Shalev SA, Shalev E, Reich D, Borochowitz ZU (1999) Osteosclerosis, hypoplastic nose, and proptosis (Raine syndrome): further delineation. Am J Med Genet 86:274–277
9. Mahafza T, El Shanti H, Omari H (2001) Raine syndrome: report of a case with hand and foot anomalies. Clin Dysmorphol 10:227–229
10. Al-Gazali LI, Jehier K, Nazih B, Abtin F, Haas D, Sadagahatian R (2003) Further delineation of Raine syndrome. Clin Dysmorphol 12:89–93
11. Hulskamp G, Wieczorek D, Rieder H, Louwen F, Hornig-Franz I, Rickert CH, Horst J, Harms E, Rehder H (2003) Raine syndrome: report of a family with three affected sibs and further delineation of the syndrome. Clin Dysmorphol 12:153–160
12. Acosta AX, Peres LC, Chimelli LC, Pina-Neto JM (2000) Raine dysplasia: a Brazilian case with a mild radiological involvement. Clin Dysmorphol 9:99–101
13. Chenna R, Sugawara H, Koike T, Lopez R, Gibson TJ, Higgins DG, Thompson JD (2003) Multiple sequence alignment with the Clustal series of programs. Nucleic Acids Res 31:3497–3500
14. Nalla VK, Rogan PK (2005) Automated splicing mutation analysis by information theory. Hum Mutat 25:334–342
15. Nalbant D, Youn H, Nalbant SI, Sharma S, Cobos E, Beale EG, Du Y, Williams SC (2005) FAM20: an evolutionarily conserved family of secreted proteins expressed in hematopoietic cells. BMC Genomics 6:11
16. Hao J, Narayanan K, Muni T, Ramachandran A, George A (2007) Dentin matrix protein 4, a novel secretory calcium-binding protein that modulates odontoblast differentiation. J Biol Chem 282:15357–15365